EFFECT OF DOPING IN *n-ZrNiSn* INTERMETALLIC SEMICONDUCTOR WITH *Bi* DONOR IMPURITY ON THERMOELECTRIC POWER FACTOR *Z**

V.A. Romaka[1,2], Yu.V. Stadnyk[3], P. Rogl[4], V.V. Romaka[2], E.K. Hlil[5], O.I. Lakh[6], A.M. Horyn[3]

([1]Ya. Pidstryhach Institute for Applied Problems of Mechanics and Mathematics, NAS of Ukraine, 3-b, Naukova Str., Lviv, 79060,Ukraine;

[2]National University "Lvivska Polytechnika", 12, Bandera Str., Lviv, 79013, Ukraine;

[3]Ivan Franko National University of Lviv, 6, Kyryla and Mefodiya Str.,79005 Lviv, Ukraine;

[4]Institut für Physikalische Chemie, Universität Wien, 42, Wahringerstrasse, Wien, A-1090, Austria;

[5]Institut Néel, CNRS, BP 166, 25, Ave. des Martyrs Grenoble Cedex 9, 38042, France;

[6]V.I. Lakh NVO "Termoprylad", 3, Naukova str., Lviv, 79060, Ukraine)

• *The structural, energy state, electrokinetic and magnetic characteristics of the n-ZrNiSn intermetallic semiconductor heavily doped with Bi were investigated. It was shown that the obtained $ZrNiSn_{1-x}Bi_x$ thermoelectric material has high efficiency of thermal into electrical energy conversion in the $T = 80 \div 400$ K temperature range.*

Introduction

Growing interest in the undoped and doped intermetallic semiconductors of *MgAgAs* (*ZrNiSn*, *TiNiSn*, *HfNiSn*, *TiCoSb*) structural type is due to equally high values of their electrical conductivity (σ) and the Seebeck coefficient (α) which, in turn, assures high efficiency of thermal into electrical energy conversion and makes these semiconductors the best studied new thermoelectric materials [1-5]. In the proposed work which contributes to further research on the effect of heavy doping (N_A, $N_D \sim 10^{19} \div 10^{21}$ cm^{-3}) of this class of semiconductors on their structural, energy state, electrophysical and magnetic properties, conditions for the origination of maximum thermoelectric power factor Z^* ($Z^* = \alpha^2 \cdot \sigma$) in *n-ZrNiSn* on doping with *Bi* donor impurity have been determined. Analysis has been performed on the peculiarities of change in crystalline and electronic structures, the temperature dependences of electrical resistivity, the Seebeck coefficient and magnetic susceptibility (χ) of $ZrNiSn_{1-x}Bi_x$ semiconductor solid solution in the range of *Bi* impurity concentrations that corresponds to $x = 0 \div 0.10$ compositions. Techniques for the fabrication of samples, structural studies, band structure calculation, kinetic and magnetic characteristics are described in [4].

Research on $ZrNiSn_{1-x}Bi_x$ crystalline structure

For a precision specification of $ZrNiSn_{1-x}Bi_x$ unit cell periods and determination of crystallographic parameters: atom coordinates, thermal parameters, occupancy of crystallographic positions, we used data sets obtained both by powder methods on automatic diffractometer Guinier-Huber image plate system ($CuK\alpha_1$; $8° \leq 2\theta \leq 100$) subject to the existence of *Ge* reference ($a_{Ge} = 0.565791$ nm) and by single-crystal methods (Enraf-Nonius CAD-4 diffractometer, MoK_α-radiation). All calculations relating to crystalline structure interpretation and specification were made with the use of WinCSD program package [6]. The phase and chemical composition of samples was controlled via electron microscopy and microprobe analysis (JEOL-840A scanning electron microscope).

The *X*-ray phase and structural analyses have shown that the investigated $ZrNiSn_{1-x}Bi_x$ samples are single-phase (*MgAgAs* structural type, ($F\bar{4}3m$) space group): the *X*-ray diffraction patterns lack reflections that might be identified with uncontrolled phases, and $ZrNiSn_{1-x}Bi_x$ crystalline structure is an ordered one. The picture of $ZrNiSn_{1-x}Bi_x$ sample surface points to the homogeneity of obtained samples (Fig. 1). The results of research on a change in *Sn* atoms concentration are the experimental evidence of the fact that in $ZrNiSn_{1-x}Bi_x$ there is a monotonous and forecasted substitution of *Sn* atoms by *Bi* atoms (Fig. 2).

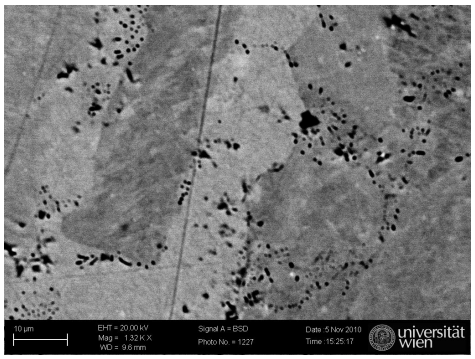

Fig. 1. $ZrNiSn_{1-x}Bi_x$ surface (magnification × 1320).

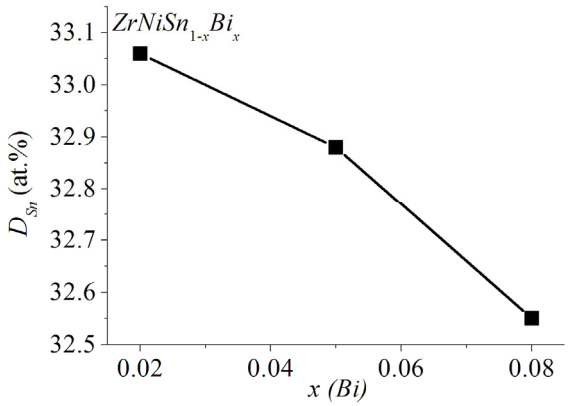

Fig. 2. Change in the values of Sn atoms concentration in $ZrNiSn_{1-x}Bi_x$.

Our previous investigations have shown that *n-ZrNiSn* crystalline structure is a disordered one [7], which is due to partial occupancy of smaller-size *Ni* atoms (r_{Ni} = 0.124 nm) of the crystallographic position of *Zr* atoms (r_{Zr} = 0.160 nm). In work [4] it is shown that with the introduction into *ZrNiSn* compound structure of weak concentrations of large-size atoms, for instance, rare-earth metals by the substitution of *Zr* or In atoms, and *Sb* by the substitution of *Sn* atoms, the impurity atoms have a different effect on the degree of order and stability of semiconductor crystalline structure. Without getting into details that can be found in [4], note that with the substitution of weak concentrations of *Sn* atoms by In and *Sb* atoms, there was no ordering of semiconductor crystalline structure.

On introducing into *ZrNiSn* compound structure of *Bi* impurity atoms by the substitution of *Sn* atoms, one could expect a monotonous increase of unit cell parameter values in $ZrNiSn_{1-x}Bi_x$. However, as we can see from Fig. 3 *a*, introduction into *ZrNiSn* compound structure of least attainable concentrations of *Bi* atoms (x = 0.005) leads to a drastic decrease of unit cell parameter values. This result, at first glance, is not logical, because the atomic radius of *Bi* (r_{Bi} = 0.170 nm) is larger than that of *Sn* (r_{Sn} = 0.158 nm) that must be attended with increase in $a(x)$ values. This, in turn, allows casting doubt upon the order of crystalline structure of $ZrNiSn_{0.995}Bi_{0.005}$ sample. At *Bi* impurity concentrations corresponding to $ZrNiSn_{1-x}Bi_x$ compositions $x > 0.005$, the values of $a(x)$ increase in a predicted manner, and the order of semiconductor crystalline structure is beyond question

With regard to the fact that *Zr*, *Sn* and *Bi* elements have close values of atomic radii, a hypothetical occupation by *Bi* atoms of *Zr* and/or *Ni* crystallographic positions would lead to increase of $ZrNiSn_{1-x}Bi_x$ $a(x)$ values, but at no event to their reduction. The established reduction of $a(x)$ values for $ZrNiSn_{0.995}Bi_{0.005}$ sample is possible only with occupation by smallest-size *Ni* atoms of *Zr* and/or *Sn* crystallographic positions. In both cases, such a substitution would generate in a crystal the donor-nature structural defects differing from such at the substitution of *Sn* atoms by *Bi*. In that event, on the temperature dependences of $ZrNiSn_{1-x}Bi_x$ kinetic coefficients we have the right to expect their manifestation in the form of several activation regions as a result of activation of electrons from two different impurity levels into semiconductor conduction band. Looking ahead, we should note that this

assumption has found its empirical support.

Crystal-chemical analysis has also shown that *Ni-Sn(Bi)*, *Zr-Sn(Bi)* and *Ni-Zr* interatomic distances are smaller than the sum of respective atomic radii (Fig. 3 *b*). However, this change as regards an undoped compound is minor. This is due to the fact that the dominating factor governing *Bi* solubility in *ZrNiSn* is the difference in the electronic structure of *Sn* and *Bi* atoms, namely in the configuration of external electronic levels. *Bi* atoms, unlike *Sn* atoms, are not characterized by sp^3 hybridization, and valence IV is apparent in compounds with a big difference in electronegativities. That is why the substitution of *Sn* by *Bi* leads to *MgAgAs* type structure destruction, and the solubility itself will be very slight. With regard to semiconductor properties of *ZrNiSn* compound, the substitution of *Sn* ($5s^25p^2$) atoms by *Bi* ($6s^26p^3$) atoms is attended with generation of donor-nature structural defects and metallization of $ZrNiSn_{1-x}Bi_x$ conductivity.

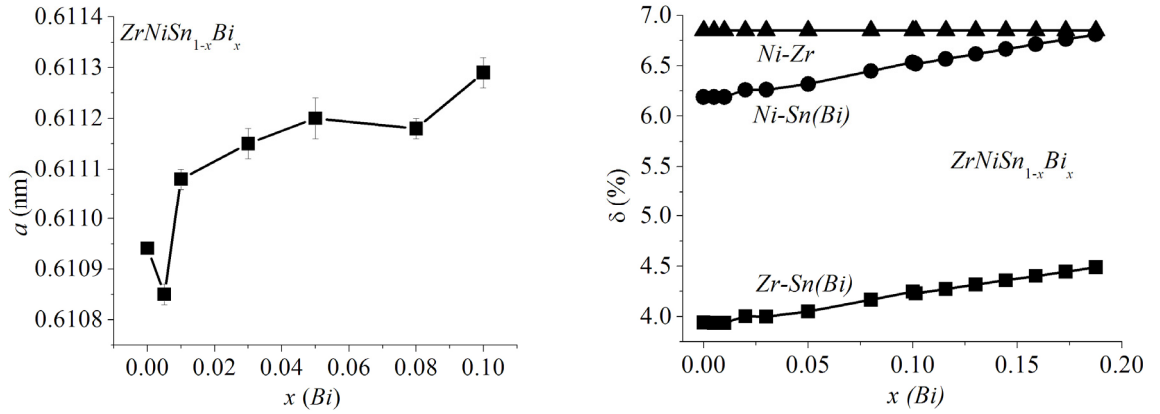

a) *b)*

Fig. 3. Change in the values of unit cell parameter a(x) (a) and relative reduction of interatomic distances δ(x) (b) in the $ZrNiSn_{1-x}Bi_x$ crystalline structure.

As long as *Bi* atoms occupy the same crystallographic position, this enables to dope a semiconductor with high precision and to obtain $ZrNiSn_{1-x}Bi_x$ material with the preassigned characteristics within the concentration range of $x = 0 \div 0.10$. Hence, merely on the basis of structural study, we can forecast the reproducibility and stability of $ZrNiSn_{1-x}Bi_x$ solid solution properties, which will enable control over the basic physical regularities of transform functions of *n-ZrNiSn*-based thermoelectric materials.

Research on $ZrNiSn_{1-x}Bi_x$ density of states distribution

To forecast the Fermi level behaviour, the electrical conductivity, the Seebeck coefficient and magnetic susceptibility values on doping of *n-ZrNiSn* intermetallic semiconductor with *Bi* impurity, the electron density distribution was calculated (Korringa-Kohn-Rostocker method in the coherent potential and local density approximations). Taking into account that doping of *n-ZrNiSn* with *Bi* impurity puts in order the crystalline structure, calculations were made for the case of ordered $ZrNiSn_{1-x}Bi_x$ crystalline structure. Fig. 4 shows the results of calculations of the electron density distribution in $ZrNiSn_{1-x}Bi_x$ for *Bi* atoms concentration: $x = 0$, $x = 0.005$, $x = 0.05$, $x = 0.10$.

The substitution of *Sn* by *Bi* atoms does not change the observed form of electron density distribution in conformity with strong hybridization between all the elements. Doping of *n-ZrNiSn* with Bi donor impurity is attended with the Fermi level drift (ε_F) towards the conduction band. Under certain concentrations of *Bi* atoms, the Fermi level will intersect the bottom of conduction band and enter the band of continuous energies, i.e. there will take place dielectric-metal transition in the

conductivity (Anderson transition) [8]. Accordingly, the Seebeck coefficient values of $ZrNiSn_{1-x}Bi_x$ will not change their sign, and the electrons will remain the majority carriers. In this context, it should be noted that intersection by the Fermi level of $ZrNiSn_{1-x}Bi_x$ conduction band at certain concentration of *Bi* atoms must be attended with the fulfillment of the condition of getting maximum values of thermoelectric power factor Z^* [5]. It makes this material a promising thermoelectric with a high efficiency of thermal into electric energy conversion. The experiment must also include a reduction of activation energy values from the Fermi level to the conduction band mobility edge on drawing of the Fermi level near the bottom of the conduction band.

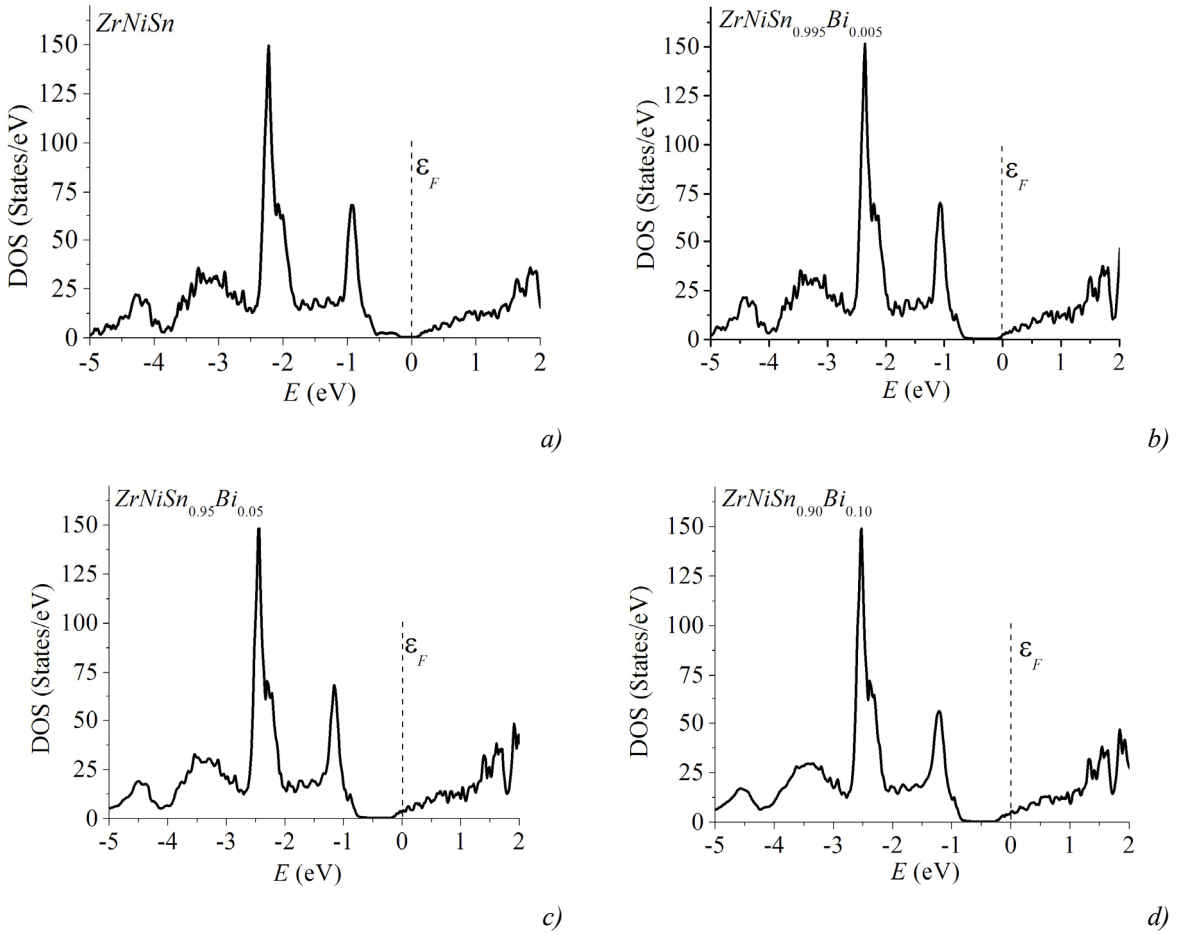

Fig. 4. Density of states distribution in $ZrNiSn_{1-x}Bi_x$.

The experimental results of research on the field and concentration dependences of $ZrNiSn_{1-x}Bi_x$ magnetic susceptibility (χ) prove the above reasoning concerning a change in semiconductor electronic state. The intermetallic semiconductor *n-ZrNiSn* is known to be a weak diamagnetic ($\chi = -0.07 \cdot 10^{-6}$ cm^3/g). The introduction of small concentrations of *Bi* atoms is attended with a change in magnetic state from a weak diamagnetic to a Pauli paramagnetic (Fig. 5). In such a case the magnetic susceptibility of $ZrNiSn_{1-x}Bi_x$ will be determined by the magnetic susceptibility of majority carriers, notably their concentration (n) (for a Pauli paramagnetic the value $\chi \sim n$). With regard to the fact that *Bi* atoms occupying the crystallographic position of *Sn* atoms generate donor-nature defects in crystal, which will lead to increased concentration of free electrons, the magnetic susceptibility values must change in a similar way. Fig. 5 represents a plot of $\chi(x)$ based on the results of $ZrNiSn_{1-x}Bi_x$ experimental investigations at $T = 300$ K and the magnetic field susceptibility $H = 0.5$ T, as well as a theoretical calculation of a change in density of states values on the Fermi level. We can see that such

dependences are similar. This and other experimental results have proved that our model of change in $ZrNiSn_{1-x}Bi_x$ crystalline structure and the results of calculation of the electron density distribution adequately reflect physical processes in the substance.

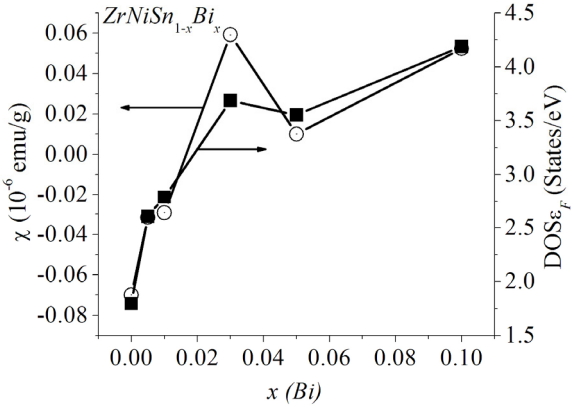

Fig. 5. Change in the values of magnetic susceptibility (χ) (experiment) and density of states at Fermi level (DOSε$_F$) in $ZrNiSn_{1-x}Bi_x$.

Thus, the above investigations of $ZrNiSn_{1-x}Bi_x$ crystalline and electronic structures have shown that doping of *n-ZrNiSn* with *Bi* impurity enables a forecast of getting thermoelectric materials with the preassigned properties, control over their characteristics, and $ZrNiSn_{1-x}Bi_x$ can be a promising thermoelectric material with stable parameters and practically appealing.

Research on $ZrNiSn_{1-x}Bi_x$ electrokinetic properties

Fig. 6 shows the temperature dependences of the electric resistivity and the Seebeck coefficient of $ZrNiSn_{1-x}Bi_x$. It can be seen that a change in the electrical resistivity values for *n-ZrNiSn* is typical for doped semiconductors with the available high- and low-temperature activation regions. Thus, in the undoped *n-ZrNiSn* semiconductor the Fermi level (ε_F) is located in the energy gap at the distance of 28.9 meV from the conduction band percolation level [4]. In that case, with a rise in temperature, under the energies larger or commensurate with the Fermi level depth of occurrence, there will be a transition of electrons from the impurity donor level to the edge of conduction band. Exactly this fact provides for the existence of high-temperature activation region on the temperature dependence $\ln\rho(1/T)$ of *n-ZrNiSn* (Fig. 6 *a*) [4]. At the same time, the availability of a low-temperature activation region testifies to the existence of a hopping mechanism of charge transfer along the localized states of impurity donor level [8]. The Fermi levels intersection and the conduction band percolation is followed by a considerable reduction of $ZrNiSn_{1-x}Bi_x$ electrical resistivity values (Fig. 7 *a*) due to increased concentration of free electrons, for instance, at 80 K, from the values of $\rho(x = 0) = 129.1$ μOhm·m to the values of $\rho(x = 0.01) = 22.49$ μOhm·m.

The introduction of least attainable in the experiment concentration of *Bi* donor impurity that corresponds to $ZrNiSn_{1-x}Bi_x$ ($x = 0.005$) composition is followed by a drastic change in the behaviour of $\ln\rho(1/T)$ dependence (Fig. 1 *a*) where three regions are clearly seen, testifying to a change of energy levels in the energy gap of such a semiconductor. Thus, at low temperatures the activation region is created as a result of electron throw from a shallow donor level (zone) with the depth of occurrence $\varepsilon_1^{\rho} = 1.3$ meV. Then, at the intermediate temperatures, on the $\ln\rho(1/T)$ dependence one can see a plateau with a small minimum, testifying to depletion of a shallow donor level (zone), namely all carriers from this level (zone) have passed to conduction band. At high temperatures, the activation region appears due to electrons transition from a different impurity donor level with the depth of

occurrence $\varepsilon_1^{\rho} = 11.5$ meV. At *Bi* concentration that corresponds to $ZrNiSn_{1-x}Bi_x$ $x \geq 0.01$ compositions the activation regions disappear, the conductivity acquires a metallic character, indicating to intersection by the Fermi level of conduction band bottom, i.e. dielectric-metal transition in the conductivity is realized which is foreseen by DOS calculations in $ZrNiSn_{1-x}Bi_x$.

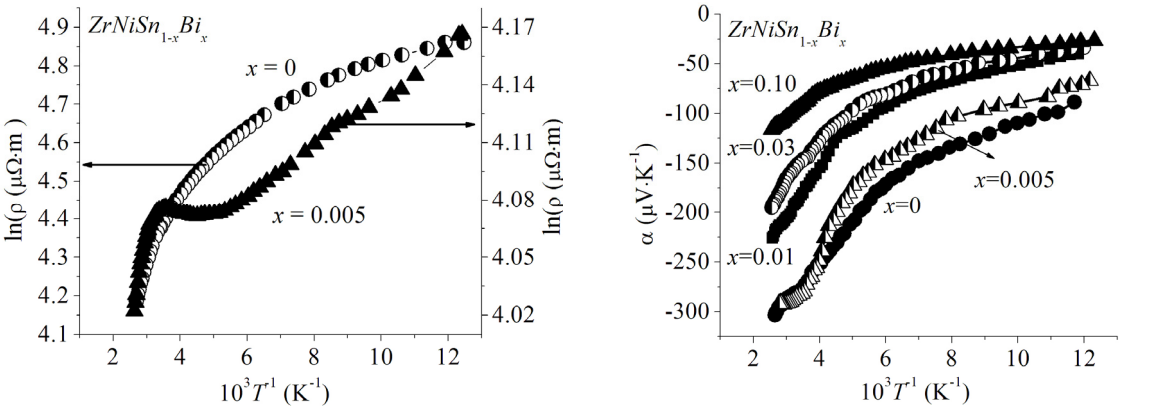

a) *b)*

Fig. 6. Temperature dependences of electrical resistivity (a) and the Seebeck coefficient (b) in $ZrNiSn_{1-x}Bi_x$.

Thus, based on the above experimental results of the temperature dependence of $ZrNiSn_{0.995}Bi_{0.005}$ electrical resistivity $\ln\rho(1/T)$, two activation regions were revealed as a result of activation of electrons from the two different impurity levels. This assumption looks logical, if we remember the results of structural analysis of $ZrNiSn_{0.995}Bi_{0.005}$ samples that have two different donor-nature structural defects. We think that this structural phenomenon became apparent on the temperature dependences of $ZrNiSn_{0.995}Bi_{0.005}$ electrical resistivity $\ln\rho(1/T)$.

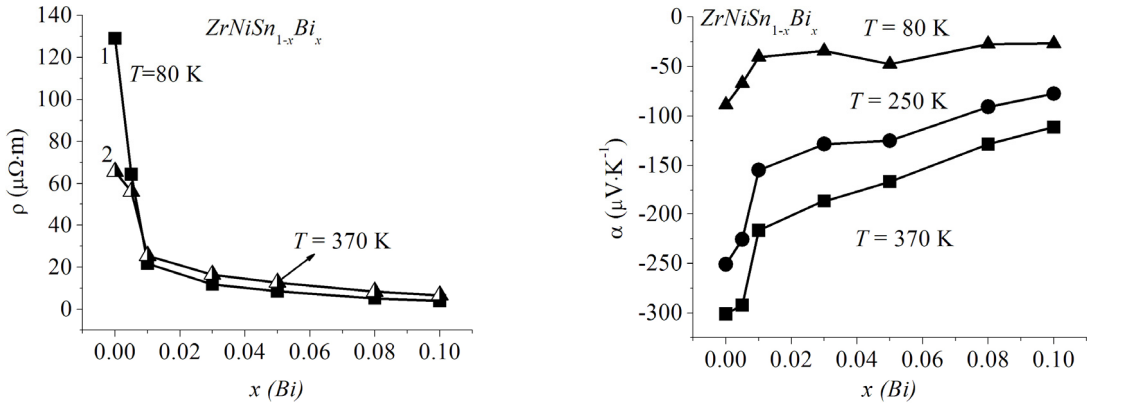

a) *b)*

Fig. 7. Concentration dependences of electrical resistivity (a) and the Seeebeck coefficient (b) in $ZrNiSn_{1-x}Bi_x$.

The fact that *Bi* impurity served as a donor is experimentally validated by the negative sign of $ZrNiSn_{1-x}Bi_x$ Seebeck coefficient (Fig. 6 *b*, 7 *b*) over the entire investigated concentration range. In turn, conduction metallization will lead to a reduction of $ZrNiSn_{1-x}Bi_x$ Seebeck coefficient values. It is conceivable that in the region of *Bi* donor impurity concentration, $x > 0.01$, which, on the one hand, will assure high electric conductivity values, and on the other hand, the Seebeck coefficient values will be still relatively high, the thermoelectric power factor of $ZrNiSn_{1-x}Bi_x$ will have an extreme point. From the high-temperature areas of $ZrNiSn_{1-x}Bi_x$ $\alpha(1/T)$ dependences (Fig. 6 *b*) we calculated the values of large-scale fluctuation amplitude of continuous energy bands (ε_1^{α}) and averaged amplitude of small-scale fluctuation potential well (ε_3^{α}) (Fig. 8). The behaviour of change in ε_1^{α} and ε_3^{α} values is

predictable. Indeed, the introduction of a donor impurity into an *n*-type semiconductor is followed by a decrease in semiconductor compensation degree [4] and, as a consequence, the fluctuation amplitude is reduced. Moreover, a correlation that has been also observed above takes place between the values of large-scale fluctuation amplitude and the depth of potential well of small-scale fluctuation: the smaller is fluctuation amplitude, the smaller is potential well of small-scale fluctuation.

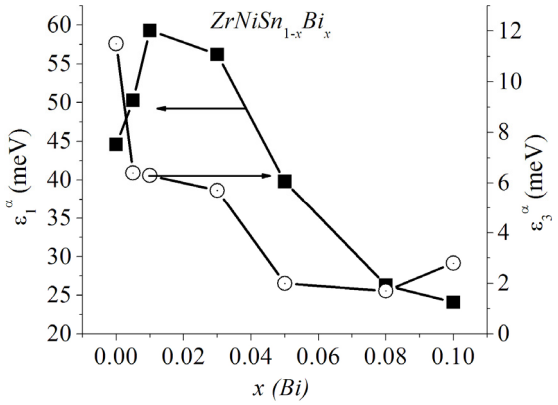

Fig. 8. Change in activation energy values $\varepsilon_1^{\alpha}(x)$ and $\varepsilon_3^{\alpha}(x)$ in $ZrNiSn_{1-x}Bi_x$.

Thus, control over the thermoelectric characteristics of *n-ZrNiSn* by doping with *Bi* donor impurity is followed by a reduction of semiconductor compensation degree, the Fermi level drift towards the conduction band percolation level, realization of dielectric-metal transition in the conductivity.

Research on $ZrNiSn_{1-x}Bi_x$ thermoelectric power factor

In work [5] it was established that a condition for origination of maximum values of thermoelectric power factor *Z** in the intermetallic semiconductors is fixation of the Fermi level by the mobility threshold of one of continuous energy bands. Taking into account that *n-ZrNiSn* is a semiconductor of electron conductivity we can assume that such a situation will be realized by introducing into the semiconductor of a small concentration of *Bi* donor impurity. Fig. 9 represents the concentration *Z*(x)* and temperature *Z*(T)* dependences of $ZrNiSn_{1-x}Bi_x$ thermoelectric power factor. The above assumption that in the region of intersection of the Fermi levels and percolation of $ZrNiSn_{1-x}Bi_x$ conduction bands there will be extreme points on the dependences of thermoelectric power factor has been verified. Therefore, the obtained $ZrNiSn_{1-x}Bi_x$ semiconductor solid solution outperforms *n-ZrNiSn* considerably and is a promising thermoelectric material.

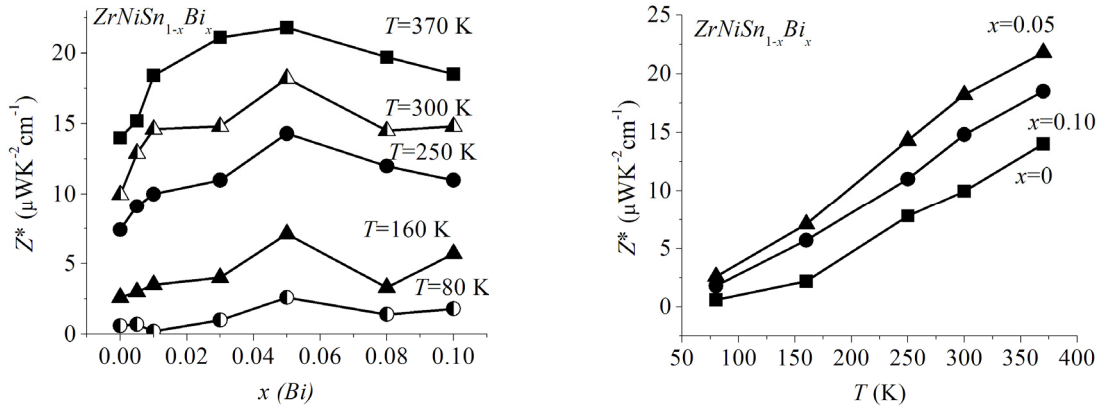

Fig. 9. Concentration (a) and temperature (b) dependences of thermoelectric power factor Z in $ZrNiSn_{1-x}Bi_x$.*

Conclusions

Thus, as a result of integrated research on the crystalline structure, energy spectrum, electrokinetic and magnetic properties of *n-ZrNiSn* intermetallic semiconductor heavily doped with donor impurity *Bi*, we have managed to predict and obtain a new promising thermoelectric material $ZrNiSn_{1-x}Bi_x$ which outperforms *n-ZrNiSn* considerably.

The work was performed in the framework of grants of the National Academy of Sciences of Ukraine (№ 0106U000594) and Ministry of Education and Science, Youth and Sports of Ukraine (№ DR 0111U001088).

References

1. S.R. Culp, S.J. Poon, N. Hickman, T.M. Tritt and J. Blumm, Effect of Substitutions on the Thermoelectric Figure of Merit of Half-Heusler Phases at 800 °C, *Appl. Phys. Letters* **88** (16), 042106-1-3 (2006).
2. Y. Kawaharada, H. Uneda, H. Muta, K. Kurosaki, S. Yamanaka, High Temperature Thermoelectric Properties of *NiZrSn* Half-Heusler Compounds, *J. of Alloys and Compounds* **364,** 59 (2004).
3. C. Uher, J. Yang, S. Hu, D.T. Morelli and G.P. Meisner, Transport Properties of Pure and Doped *MNiSn* (*M = Zr, Hf*), *Phys. Rev. B* **59**(13), 8615 (1999).
4. V.A. Romaka, V.V. Romaka, Yu.V. Stadnyk, *Intermetallic Semiconductors: Properties and Applications* (Lvivska Polytechnika, 2011).
5. V.A. Romaka, D. Fruchart, Yu.V. Stadnyk, J. Tobola, Yu.K. Horelenko, M.G. Shelyapina, L.P. Romaka and V.F. Chekurin, Conditions for the Attainment of Maximum Values of Thermoelectric Power Factor in the Intermetallic Semiconductors of *MgAgAs* Structural Type, *Fiz.Tekhn.Polupr*. **40** (11), 1309 (2006).
6. L.G. Akselrud, Yu.N. Grin, P.Yu. Zavali, V.K. Pecharsky and V.S. Fundamenskii, CSD – Universal Program Package for Single Crystal or Powder Structure Data Treatment, *12th Eur. Crystallogr. Meeting*, *Collected Abstracts*, Vol. 3, p. 155 (Nauka, Moscow, 1989).
7. V.A. Romaka, D. Fruchart, E.K. Hlil, P.E. Gladyshevsky, D. Gignoux, V.V. Romaka, B.S. Kuzhel and R.V. Krayovsky, Peculiarities of *n-ZrNiSn* Intermetallic Semiconductor Heavily Doped with Atoms of Rare-Earth Metals, *Fiz.Tekhn.Polupr*. **44**(3), 310 (2010).
8. N.F. Mott, E.A. Davis, *Electron Processes in Non-Crystalline Materials* (Nauka, Moscow, 1982) (Transl. from English: N.F. Mott, E.A. Davis, Electron Processes in Non-Crystalline Materials, Oxford, Clarendon Press, 1979).
9. B.I. Shklovsky, A.L. Efros, Transition from Metallic to Activation Conductivity in Compensated Semiconductors, *JETF* **61** (2), 816 (1971).
10. B.I. Shklovsky, A.L. Efros, Fully Compensated Crystalline Semiconductor as a Model of Amorphous Semiconductor, *JETF*, **62** (3), 1156 (1972).

Submitted 31.10.2011